Experimental determination of pair interactions in a $Fe_{0.804}V_{0.196}$ single crystal

V. Pierron-Bohnes, E. Kentzinger, and M.C. Cadeville
Institut de Physique et de Chimie des Matériaux de Strasbourg–Groupe d'Etude des Matériaux Métalliques, CNRS, Université Louis Pasteur, 23 rue du Loess, 67037 Strasbourg, France

J.M. Sanchez
Center for Materials Science and Engineering, University of Texas, Austin, Texas 78712

R. Caudron and F. Solal
Office National d'Etudes et de Recherches Aérospatiales, 29 avenue de la Division Leclerc, 92320 Châtillon-sous-Bagneux and Léon Brillouin Laboratory (LLB), CEN Saclay, 91190 Gif-sur-Yvette, France

R. Kozubski
Institute of Physics, Jagellonian University, Reymonta 4, 30-059 Krakow 16, Poland
(Received 14 September 1994)

The short-range order in a $Fe_{0.804}V_{0.196}$ single crystal at 1133 and 1473 K was measured using neutron diffuse scattering in the [100] and [110] planes. The data were used in conjunction with the inverse cluster-variation method in order to extract the first five effective-pair-interaction potentials V_1 to V_5. The interactions obtained from the experimental short-range-order intensities are compared with the results of different theoretical calculations.

I. INTRODUCTION

Recent theoretical and computational developments in alloy theory have made possible the nonempirical calculation of phase diagrams and, in general, the study of phase stability strictly from first principles. In the case of phase diagrams, the results depend crucially on the values of atomic interactions which, in turn, are usually obtained invoking numerous and different levels of approximations. At present, several methods aimed at extracting interactions have been proposed. Among the approaches most commonly used are the generalized perturbation method,[1–4] in which the interactions are obtained by perturbation of the random alloy, and the method of Connolly and Williams,[5] which is based on the cluster expansion method.[6,7] Some of these approaches have been successfully used to calculate complete and relatively accurate binary[8–16] and ternary[17] phase diagrams. For the specific case of the Fe-V system, phenomenological models[18] and electronic structure calculations[18–22] have also been used in order to obtain pair interactions.

Parallel to the theoretical studies, significant effort has been devoted to the experimental determination of the effective interactions in alloys. These studies have focused on the examination of single crystals in thermodynamic equilibrium for systems where the phase diagram is well known and relatively simple such as Cu-Au,[23,24] Ni-V,[25,26] Pd-V,[25,26] Ni-Cr,[27–30] Ni-Al,[31] and Fe-Al.[32–34]

The system investigated here, Fe-V, offers some interesting aspects. First, the Fe-V phase diagram exhibits a *metastable* $B2$-ordered phase extending around equiatomic concentration. At low temperatures the system transforms to a σ phase, although the transformation is sufficiently sluggish so that the disordered-$B2$ transition is well characterized.[35] We note that the presence of the $B2$ phase is determined primarily by the effective pair interactions. Second, although some diffuse intensity measurements have been carried out in Fe-V, such measurements were performed using polycrystalline material,[36] or samples that were too small to provide accurate data,[37] or with samples that were not in thermodynamic equilibrium.[38] Thus, there is a need for accurate diffuse intensity measurements in this system. Finally, theoretical estimates of the effective pair interactions in this system are available[18–22] and, thus, comparison with reliable experimental data would be desirable.

Here we describe high-temperature neutron diffuse scattering measurements on a $Fe_{0.804}V_{0.196}$ single crystal. First we present a brief summary of the experimental procedure, followed by a description of the results in terms of short-range-order (SRO) parameters. In Sec. III, effective pair interactions are calculated using the inverse cluster variation method and the results are discussed in the context of available electronic structure calculations. Concluding remarks are presented in Sec. IV.

II. EXPERIMENTAL PROCEDURE

The sample, provided by Perrier de la Bathie (Grenoble, France), consisted of a cylindrical single crystal 3 cm long and 5 mm in diameter oriented along the [850] direction. The sample was annealed for 8 days at 1113 K under a 10 Torr vacuum. Its composition, determined by atomic absorption analysis, was 19.6 ± 1 at. % vanadium.

The diffuse intensity measurements were carried out with the G44 instrument of the Léon Brillouin Laboratory. This two-axis spectrometer is equipped with 48 detectors placed every 2.5°, between 8° and 128°. This particular layout gave access to 48 reciprocal space points of the Ewald circle situated on the scattering plane. By rotating the sample in steps of 4°, we scanned a large region of the scattering plane. For the incident wavelength used (0.259 nm), the scanned region was contained between the circles of radii 0.35 and 2.1 reciprocal lattice units (RLU), with a sampling mesh of 1600–2000 measurement points. Three-dimensional information was obtained by tilting the single crystal by 14° and 32°, which allowed measurements to be carried out on the (110) and (100) planes, respectively.

The measurements were taken at 1133 and 1473 K using a high-temperature furnace located at the center of a 80 cm vacuum vessel. Placing the crystal under vacuum results in significant reduction of the background intensity. At the temperatures investigated, which fall above the Curie temperature of the alloy, thermodynamic equilibrium is reached within a second.[39] However, phonon annihilation processes play an important role and an energy analysis is necessary in order to reject their contribution to the measured intensity. This energy analysis was performed using a time-of-flight system. Moreover, in Fe-V, a small critical magnetic scattering contribution is expected[40] which, however, can be also eliminated by the time-of-flight analysis. Typical time-of-flight spectra are shown in Fig. 1. Due to the long incident wavelength, the dominant process is phonon absorption, except in the close vicinity of the Bragg peaks. Thus, the spectra show inelastic scattering essentially on the high-energy side (left side of Fig. 1). This background intensity was eliminated using an exponential function superimposed onto the typical trapezoidal form of the elastic contribution, which was obtained measuring a vanadium probe at room temperature. The points containing both creation and absorption of phonons or visible magnetic critical contributions were discarded.

The scattering cross sections were deduced from the area of the elastic contribution with standard corrections for instrumental background (empty furnace) and multiple scattering. Calibration was carried out by comparison with the incoherent scattering of a vanadium probe having the same shape, dimensions, and position in the furnace. Some detectors gave erratic results near the polycrystalline peaks of the furnace and, therefore, the corresponding data points were eliminated.

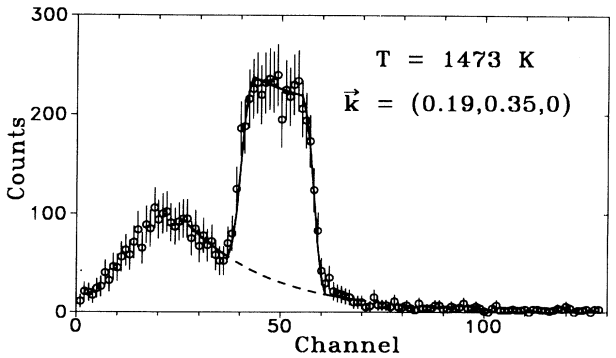

FIG. 1. Typical time-of-flight spectrum in $Fe_{0.804}V_{0.196}$ and the corresponding fit: The inelastic contribution and the total cross section obtained in the fit are shown in dashed and solid lines, respectively.

The Debye-Waller factors were evaluated using short-wavelength neutron diffraction performed on a powder sample of the same composition as the single crystal. A cryostat (5–300 K) and a vacuum furnace (300–1200 K) were used to scan a large temperature range (Fig. 2). The obtained Debye-Waller factors were extrapolated to the temperatures at which the scattering experiments were conducted to correct the SRO intensity data for thermal attenuation.

The absorption corrections were evaluated by approximating the sample to a vertical cylinder with the same cross section. Since the linear absorption coefficients of $Fe_{0.804}V_{0.196}$ and vanadium are similar and since their cross sections appear as a ratio due to the normalization of the sample cross section by the vanadium one, the corresponding final correction is not large.

The incoherent scattering of the sample was calculated using $\sigma_{\rm inc}^{\rm Fe} = 0.40(11)$ barn and $\sigma_{\rm inc}^{\rm V} = 5.08(6)$ barns for the incoherent scattering cross sections of Fe and V, respectively.[41] Hence, for the alloy we have $\sigma_{\rm inc}^{\rm alloy} = 1.32 \pm 0.15$ barn. The Laue cross section is $4\pi F_{\rm Laue} = 1.914 \pm 0.08$ barn where $F_{\rm Laue}$ is the usual normalization factor given by $F_{\rm Laue} = c(1-c)(b_{\rm V} - b_{\rm Fe})^2$, with c the vanadium concentration, and $b_{\rm V}$ and $b_{\rm Fe}$ the coherent scattering lengths of V and Fe, respectively. The incoherent scattering is thus expected to be 0.69 ± 0.11 in Laue units (LU).

III. SHORT-RANGE-ORDER PARAMETERS

The experimental cross sections at the two temperatures investigated here are shown in Fig. 3. Although there is a noticeable decrease in SRO with temperature, SRO is still significant at 1473 K. The measured intensity

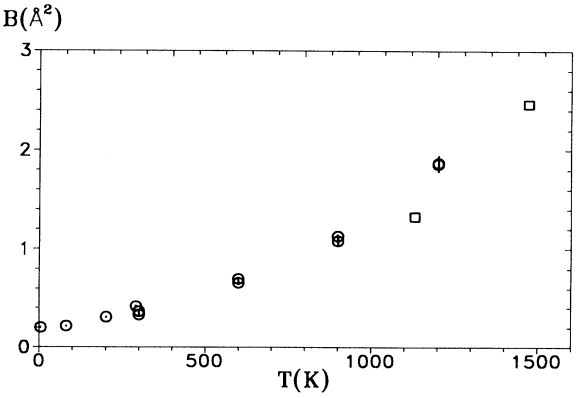

FIG. 2. Temperature dependence of the coefficient B (Å^2) used for the Debye-Waller attenuation factor $[\exp(-B \sin^2\theta/\lambda^2)]$. Values obtained from the Bragg peaks of a $Fe_{0.804}V_{0.196}$ powder (○) and final values used in the correction of the SRO intensity (□).

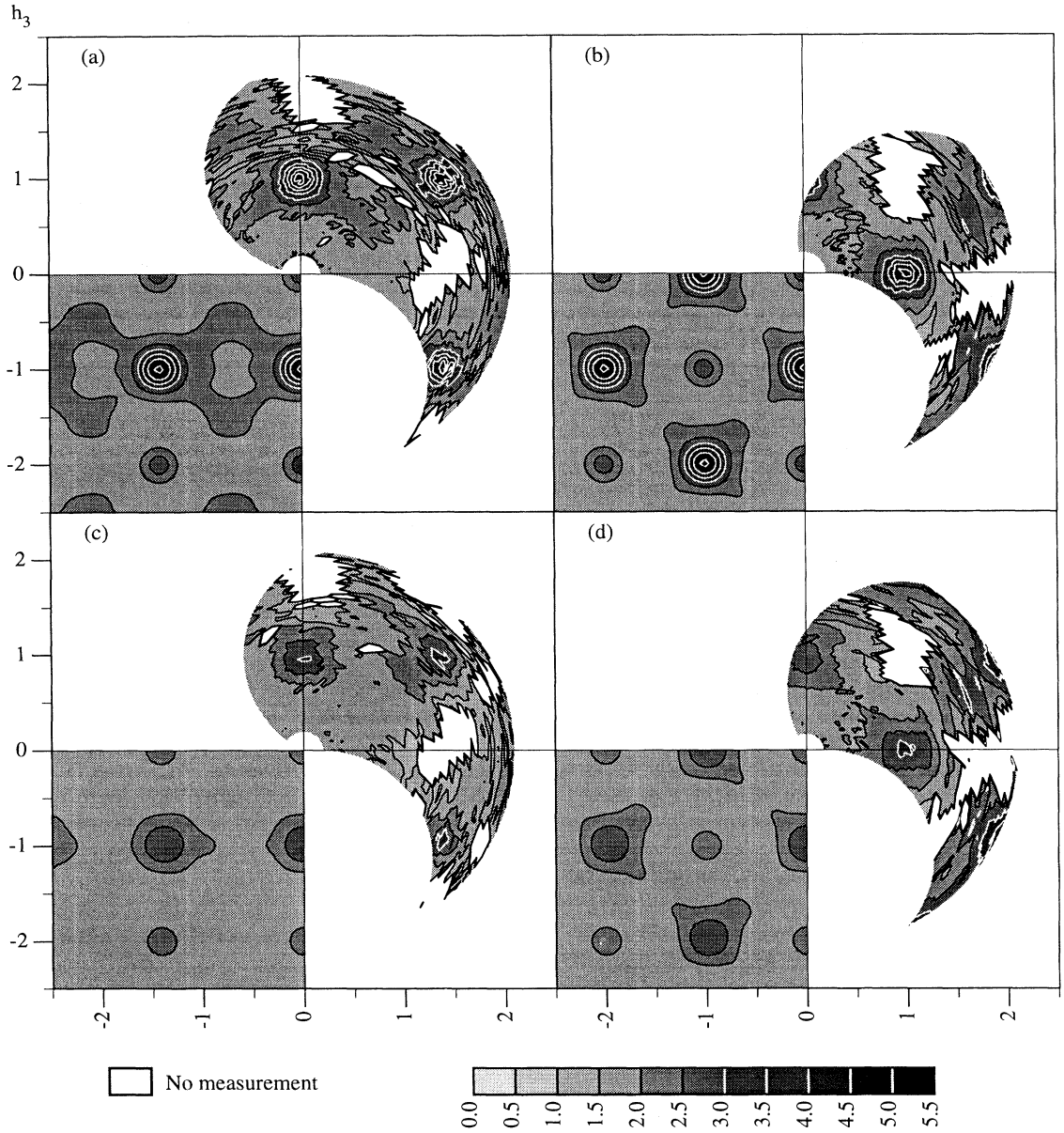

FIG. 3. Corrected experimental intensities and calculated ones in the [110] (a),(c) and [100] (b),(d) planes, at 1133 K (a),(b) and 1473 K (c),(d). In each panel, the simulation (down left) has to be compared to the measurement taking into account the symmetries of the plane.

is mostly concentrated near the [100] and [111] equivalent points and, within the experimental errors, the intensity is zero at $[\frac{1}{2}\frac{1}{2}\frac{1}{2}]$. The static displacements are small, giving rise to a weak asymmetry of the diffuse peaks.

The cross sections were analyzed using the Borie-Sparks[42] formulation. In terms of the measured scattering cross section, with corrections for temperature attenuation given by the Debye-Waller factor B, the corrected intensity in Laue units is written

$$I_{\mathrm{corr}}(\mathbf{k}) = \frac{1}{NF_{\mathrm{Laue}}}\left[\frac{d\sigma}{d\Omega}(\mathbf{k})e^{(Bk^2/8\pi^2)}\right], \qquad (1)$$

where N is the total number of atoms.

Up to first order in the atomic displacements $\mathbf{u_p}$ at lattice site $\mathbf{R_p} = \frac{a}{2}(p_1, p_2, p_3)$, where $\mathbf{p}$ stands for the set of integers (p_1, p_2, p_3), the corrected intensity at the reciprocal space point $\mathbf{k} = \frac{2\pi}{a}(h_1, h_2, h_3)$ is given by

$$I_{\mathrm{corr}}(\mathbf{k}) = \alpha(\mathbf{k}) + \sum_{i=1}^{3} h_i Q_i(\mathbf{k}) + I_{\mathrm{inc}}, \qquad (2)$$

where $\alpha(\mathbf{k})$ is the SRO contribution, the $Q_i(\mathbf{k})$ are related to the Fourier transform of the atomic displacements, and I_{inc} is the incoherent scattering per atom in Laue units.

The SRO intensity is given by the Fourier transform of the Warren-Cowley SRO parameters $\alpha_{\mathbf{p}}$:[43]

$$\alpha(\mathbf{k}) = \sum_{\mathbf{p}} \alpha_{\mathbf{p}} \cos(\mathbf{k}\cdot\mathbf{R_p}), \qquad (3)$$

with the Warren-Cowley SRO parameters defined by

$$\alpha_{\mathbf{p}} = \frac{\langle \sigma_{\mathbf{o}} \sigma_{\mathbf{p}} \rangle - \langle \sigma_{\mathbf{o}} \rangle^2}{1 - \langle \sigma_{\mathbf{o}} \rangle^2}, \tag{4}$$

where $\sigma_{\mathbf{o}}$ and $\sigma_{\mathbf{p}}$ are occupation operators at the origin and site $\mathbf{p}$, respectively. These occupation operators take values 1 or -1 if the lattice site is, respectively, occupied by Fe or V atoms, and the brackets $\langle\ \rangle$ stand for configurational averages.

The quantities $\mathbf{Q}(\mathbf{k}) = [Q_1, Q_2, Q_3]$ in Eq. (2) are given by the first-order displacement parameters $\gamma_{\mathbf{p}}$:

$$\mathbf{Q}(\mathbf{k}) = \sum_{\mathbf{p}} \gamma_{\mathbf{p}} \sin(\mathbf{k} \cdot \mathbf{R}_{\mathbf{p}}). \tag{5}$$

In turn, the displacement parameters $\gamma_{\mathbf{p}}$ are defined by

$$\gamma_{\mathbf{p}} = -\frac{2\pi}{a} \sum_{\sigma\sigma'} \frac{b_\sigma b_{\sigma'}}{F_{\text{Laue}}} \rho_{2,\mathbf{p}}(\sigma\sigma') \langle \Delta \mathbf{u}_{\mathbf{p}}^{\sigma\sigma'} \rangle, \tag{6}$$

where $\langle \Delta \mathbf{u}_{\mathbf{p}}^{\sigma\sigma'} \rangle$ is the average relative displacement between atoms of type σ and σ' (i.e., Fe or V) separated by $\mathbf{R}_{\mathbf{p}}$, and where $\rho_{2,\mathbf{p}}(\sigma\sigma')$ is the probability of finding atoms σ and σ' at a distance $\mathbf{R}_{\mathbf{p}}$. We note that these probabilities are $c^2 + c(1-c)\alpha_{\mathbf{p}}$, $(1-c)^2 + c(1-c)\alpha_{\mathbf{p}}$, and $c(1-c) - c(1-c)\alpha_{\mathbf{p}}$ for V-V, Fe-Fe, and Fe-V pairs, respectively.

A set of Warren-Cowley SRO parameters and of first-order displacement parameters were fitted to the corrected data using a least-squares procedure with a weight inversely proportional to the square of the experimental error ΔI. Thus, the residual error to be minimized is

$$\chi^2 = \sum \frac{(I_{\text{measured}} - I_{\text{calculated}})^2}{N_{\text{freedom}} \Delta I^2}, \tag{7}$$

where $N_{\text{freedom}} = N_{\text{points}} - N_{\text{variables}}$ is the number of degrees of freedom of the fit, and N_{points} is the number of experimental points (around 3000).

We have varied the number of shells for the SRO parameters up to 20, and those for the displacements up to 8. The sensitivity of the results to the number of SRO shells is shown in Fig. 4. Above 9 SRO parameters, the residual error does not vary significantly and all the calculated cross sections are qualitatively the same, indicating that the parameters are stable. At 1133 K, the diffuse signal is a little sharper with 20 shells than with 9 shells whereas at 1473 K there is no difference. With regard to the displacement parameters, all results are stable above 3 shells. We will show and discuss the results analyzed with 16 shells for the SRO parameters and 3 shells for the displacement parameters.

As can be seen in Fig. 2, the powder Debye-Waller factor determination is less accurate at temperatures above 1000 K as the measured peak intensities become very weak at large angles and we have to use an extrapolation to estimate the values of B at the SRO measurement temperatures. Moreover, it is expected that the attenuations of the diffuse scattering and of the Bragg peaks are not equal in the presence of static displacements, since the sign in front of the static Debye-Waller contribution is different in the two cases.[44] To take into account a possible difference between the applied correction and the real Debye-Waller attenuation (δB), we added in Eq. (2) a term of the form $\delta_0 k^2$ (development at the second order in δB of the term $e^{(Bk^2/8\pi^2)}$) of Eq. (1) and fitted δ_0 to the experimental data. The Debye-Waller factor [B in Eq. (1)] was corrected until the value of δ_0 resulting from the fit was zero. The corresponding values of B are shown as squares in Fig. 2. As expected, they are somewhat lower than the values measured from the Bragg peak attenuation.

The values of the α_n for each shell n are given in Table I and in Fig. 5. In absolute values, the largest parameters are α_1, α_2, α_3, and α_5, with a strong repulsive parameter between nearest-neighbor like atoms and smaller attractive ones between second, third, and fifth neighbors. The signs of these SRO parameters are in agreement with the nature of the pairs observed in the $B2$-ordered phase: heterochemical first (pair of atoms 1 and 5 in Fig. 6) and fourth neighbor (1 and 6) pairs, homochemical second (1 and 2), third (1 and 3), and fifth (1 and 9) neighbor pairs.

We note that the sign of α_2 is different from that obtained in previous studies.[37,38] Since these previous measurements were performed in the ferromagnetic state, the

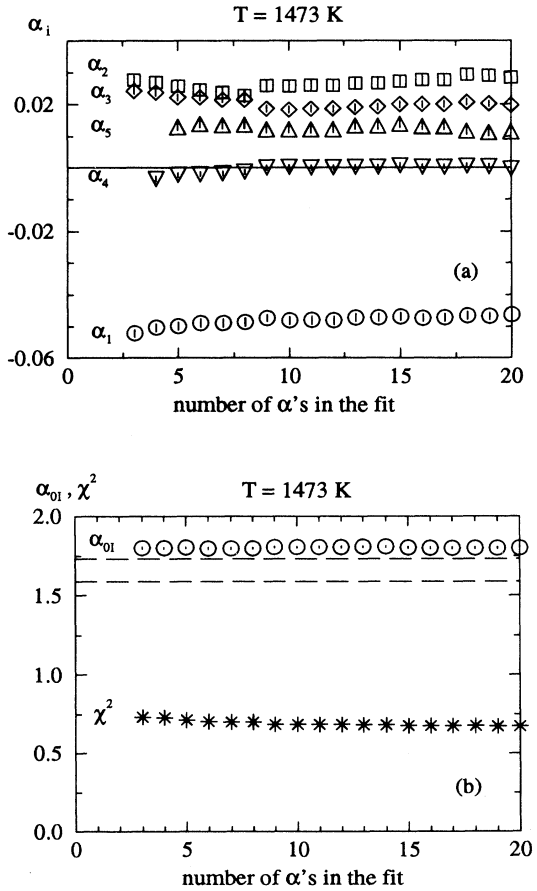

FIG. 4. Sensitivity of the SRO parameters α_n, the constant contribution α_{0I}, and the residual error χ to the number of SRO parameters in the fit.

TABLE I. Experimental short-range-order and displacement parameters at 1133 and 1473 K.

	1133 K		1473 K	
n	α_n	$\Delta\alpha_n$	α_n	$\Delta\alpha_n$
1	−0.0755	0.0023	−0.0468	0.0017
2	0.0349	0.0026	0.0282	0.0026
3	0.0468	0.0016	0.0201	0.0016
4	−0.0075	0.0015	0.0004	0.0015
5	0.0244	0.0027	0.0124	0.0026
6	0.0165	0.0019	0.0120	0.0023
7	−0.0057	0.0012	−0.0014	0.0010
8	0.0094	0.0012	0.0022	0.0012
9	0.0109	0.0011	0.0089	0.0010
10	−0.0016	0.0014	−0.0024	0.0014
11	0.0003	0.0012	0.0016	0.0009
12	0.0047	0.0016	0.0008	0.0012
13	0.0004	0.0009	0.0028	0.0007
14	0.0041	0.0011	0.0006	0.0011
15	0.0118	0.0015	0.0081	0.0016
16	−0.0015	0.0008	−0.0026	0.0010
n	γ_n	$\Delta\gamma_n$	γ_n	$\Delta\gamma_n$
1	−0.0204	0.0011	−0.0262	0.0012
2	0.0050	0.0021	0.0103	0.0025
3	0.0012	0.0011	0.0046	0.0012

discrepancy is most likely due to the effect of magnetic correlations. Furthermore, in Ref. 38, unlike the present measurements that have been carried out *in situ* at high temperatures, the samples studied were quenched from 1223 K and were not, therefore, in a state of thermodynamic equilibrium.[39] Finally, let us note that in Ref. 37 the sensitivity of the measurements was poor (e.g., $\alpha_2 = -0.023 \pm 0.026$) due to the small size of the sample.

The cross sections reconstructed using Eq. (2) are shown in Fig. 3. Taking into account the experimental errors (0.2 LU on average), the results of the simulations are in good agreement with the experimental ones. The diffuse intensity is nearly symmetrical around the [100] and [111] points, which is indicative of the fact that the displacement contributions are small in this case. This is not surprising in view of the fact that the coherent neutron scattering length of vanadium is small. Thus, the Fe-Fe term in Eq. (6) provides the main contribution to the displacement parameters. However, relative displacements of the Fe (matrix) atoms are expected to contribute mainly to the variation of the average lattice constant and not to the local distortions.

The constant contribution to the cross section, α_{0I}, is the sum of the $\alpha_0 = 1$ term and the sample incoherent contribution. Its expected value is thus 1.69 ± 0.11 LU. We obtain 1.94 ± 0.01 LU at 1133 K and 1.80 ± 0.01 LU at 1473 K, which is quite in line with the expected value considering its error bar. Some authors[25,26] attribute such a difference to a bad evaluation of the number of atoms in the beam and renormalize all the data. We consider that there is no reason to apply such a correction as the relative departure (8%) is of the order of magnitude of the relative error bars on the SRO parameters. Moreover, as the departure decreases with the temperature, this small contribution can perhaps be attributed to some magnetic short-range-order contributions.

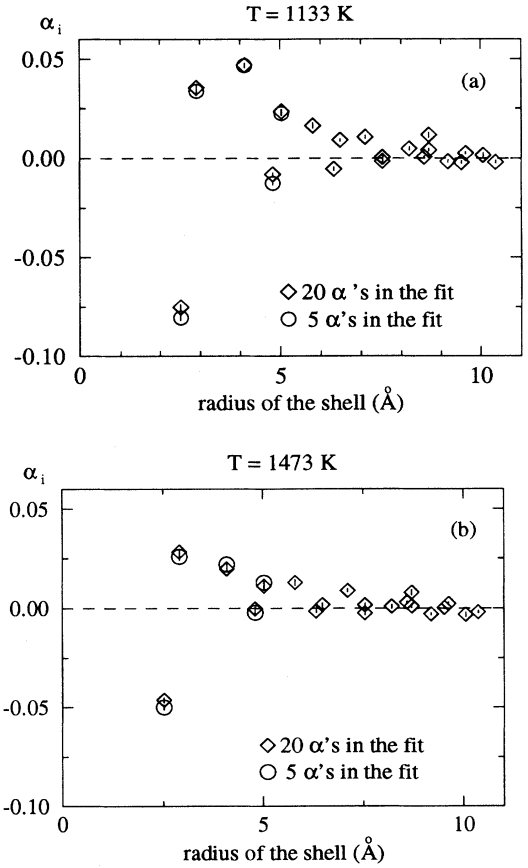

FIG. 5. Variation of the Warren-Cowley SRO parameters with the distance.

IV. EFFECTIVE PAIR INTERACTIONS

In order to extract the effective pair interactions from the experimental values of the Warren-Cowley SRO parameters, we consider a simple Ising Hamiltonian for the alloy in which the magnetic moments are localized on the Fe atoms:

$$H_0 = \frac{1}{2}\sum_{\mathbf{p},\mathbf{p}'} V^c_{\mathbf{p}\mathbf{p}'}\sigma_{\mathbf{p}}\sigma_{\mathbf{p}'} - \frac{1}{8}\sum_{\mathbf{p},\mathbf{p}'} J_{\mathbf{p}\mathbf{p}'}(1+\sigma_{\mathbf{p}})(1+\sigma_{\mathbf{p}'})S_{\mathbf{p}}S_{\mathbf{p}'}, \quad (8)$$

where $S_{\mathbf{p}} = \pm 1$ is the spin at site $\mathbf{R}_{\mathbf{p}}$. In Eq. (8), $V^c_{\mathbf{p}\mathbf{p}'}$ and $J_{\mathbf{p}\mathbf{p}'}$ are, respectively, effective chemical and exchange interactions between sites $\mathbf{R}_{\mathbf{p}}$ and $\mathbf{R}_{\mathbf{p}'}$. Averaging over the magnetic degrees of freedom, the interacting part of the alloy Hamiltonian can be written as

$$H_2 = \frac{1}{2}\sum_{\mathbf{p},\mathbf{p}'} \tilde{V}_{\mathbf{p}\mathbf{p}'}\sigma_{\mathbf{p}}\sigma_{\mathbf{p}'}, \quad (9)$$

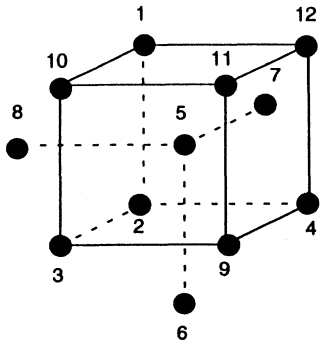

FIG. 6. Clusters used in the CRO approximation of the cluster variation method: body-centered cube (points 1–5 and 9–12), octahedron (points 2–6 and 9), and the rhombohedron (points 1–8).

where the effective pair interaction is

$$\tilde{V}_{\mathbf{pp'}} = V^{c}_{\mathbf{pp'}} - \frac{1}{4} J_{\mathbf{pp'}} \langle S_{\mathbf{p}} S_{\mathbf{p'}} \rangle . \tag{10}$$

We note that, in terms of interatomic potentials between different chemical species, the effective interactions are given by

$$\tilde{V}_{\mathbf{pp'}} = \frac{1}{4} [\tilde{V}^{\text{Fe-Fe}}_{\mathbf{pp'}} + \tilde{V}^{\text{V-V}}_{\mathbf{pp'}} - 2\tilde{V}^{\text{Fe-V}}_{\mathbf{pp'}}] . \tag{11}$$

Thus, in the present model, the unknown magnetic SRO is included in the effective pair interactions, which now should depend on temperature.[33] Furthermore, since the product $J_{\mathbf{pp'}} \langle S_{\mathbf{p}} S_{\mathbf{p'}} \rangle$ in Eq. (10) is always positive, the $\tilde{V}_{\mathbf{pp'}}$ are smaller than the chemical interactions $V^{c}_{\mathbf{pp'}}$.

In order to extract these effective interactions from the experimental diffuse scattering, we fitted the Warren-Cowley SRO parameters using the inverse cluster variation method (CVM) algorithm proposed by Gratias and Cénédèse.[45] The CVM approximation used in the inverse method includes three maximum clusters: the body-centered cube, the eight-point rhombohedron, and the octahedron shown in Fig. 6. In this approximation, which we will refer to as the CRO approximation, we are able to compute the first five effective interactions in the bcc lattice. In particular, we note that the approximation includes the fourth neighbor pairs, which have been neglected in previous applications of the inverse CVM to bcc lattices.[33,34] The results of the inverse CVM applied to $Fe_{0.804}V_{0.196}$ at the two temperatures investigated are presented in Table II.

It is apparent from the results of Table II that the effective pair interactions vary appreciably with temperature. As mentioned, this temperature dependence is most likely due to changes in the magnetic SRO [see Eq. (11)]. In the limit of high temperatures, however, the $\tilde{V}_n$ should tend to constant values as the magnetic SRO parameters $\langle S_{\mathbf{p}} S_{\mathbf{p'}} \rangle$ become negligible. This behavior has been confirmed in a recent study of the Fe-Al system, where the interplay between chemical and magnetic SRO is also present.[34] We note that the lowest temperature investigated here (1133 K) is close to the Curie temperature (T_C = 1073 K) of the $Fe_{0.804}V_{0.196}$ alloy. Thus, the effect of magnetic SRO on the pair interactions should be significant. On the other hand, the values of $\tilde{V}_n$ obtained at 1473 K are expected to be closer to the high-temperature limit.

A point of considerable interest is the comparison of the effective pair interactions obtained from diffuse intensity measurements and those calculated using electronic structure methods. At present there are several electronic structure calculations for the Fe-V system.[19–22] In particular, the interactions calculated in Ref. 20 were obtained without including spin polarization and, thus, they should be comparable to the experimental interactions derived here. The values of $\tilde{V}_n$ calculated by Sluiter and Turchi[20] for Fe_3V are listed in Table II, with the corresponding α_n at 1473 K, obtained using the CVM, given in the last column. We note that these effective interactions were determined using the generalized perturbation method and the coherent potential approximation with a tight-binding Hamiltonian. Aside from the fact that a tight-binding Hamiltonian is a questionable approximation, these authors have reported that for Fe-V the effective interactions depend strongly on off-diagonal disorder.[20] Consequently, the results for $\tilde{V}_n$ should be expected to be very sensitive to the choice of tight-binding parameters.

It is apparent from the results shown in Table II that there are significant discrepancies between the $\tilde{V}_n$, or equivalently the α_n, obtained from the diffuse intensity measurements and those calculated by Sluiter and Turchi.[20] In particular, the electronic structure results show a rapid decrease of the effective interactions with distance, whereas this is not the case for the $\tilde{V}_n$ derived from the SRO intensity. More significantly, the value of $\tilde{V}_1$ (or of $|\alpha_1|$) predicted by the electronic structure calculations is much larger than the value derived from the experimental data.

In order to further explore this discrepancy, we have also calculated the SRO intensity at 1473 K using the k-space formulation of the CVM developed by one of the present authors.[46] This k-space formulation of the CVM

TABLE II. Pair interactions for $Fe_{0.804}V_{0.196}$ from this work and for Fe_3V from Ref. 20.

	1133 K		1473 K		Ref. 20	
n	α_n	$\tilde{V}_n$ (meV)	α_n	$\tilde{V}_n$ (meV)	$\tilde{V}_n$ (meV)	α_n (1473 K)
1	−0.0755	9.8(0.4)	−0.0468	8.2(0.6)	23.0	−0.1082
2	0.0349	−1.2(0.6)	0.0282	−3.6(0.7)	2.2	0.0409
3	0.0468	−4.6(0.4)	0.0201	−2.9(0.5)	1.0	0.0271
4	−0.0075	−1.2(0.4)	0.0004	−1.2(0.4)	1.5	−0.0179
5	0.0244	−1.9(0.5)	0.0123	−1.5(0.5)	−3.2	0.0305

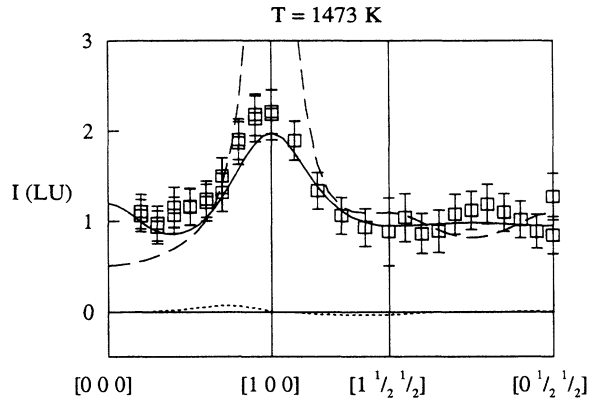

FIG. 7. Short-range-order intensity at 1473 K calculated using the k-space formulation of the cluster variation method (Ref. 46) with the effective interactions of Ref. 20 (dashed line) and those obtained in this work (solid line). Also shown are the experimental data (□). The displacement contribution is shown in dotted line.

provides a significantly improved description of the SRO intensity over the more commonly used Krivoglaz-Clapp-Moss[47–49] formula. The SRO intensities calculated using the interactions derived in this work (solid line) and those obtained by Sluiter and Turchi (dashed line) are compared to each other and to the experimental data (symbols) in Fig. 7. The calculations were carried out in the CRO approximation described previously and, therefore, all five pair interactions are used. As it might be expected from the results of Table II, the SRO intensity predicted by the electronic structure calculations is also in sharp disagreement with the experimental data. The discrepancy is particularly noticeable around the maximum at [100]. This excessively large value of SRO intensity at [100] is due to the overestimation of $\tilde{V}_1$ by the electronic structure calculations. There are also discrepancies in the general shape of the intensity, which are more likely due to errors in the predicted ratios $\tilde{V}_n/\tilde{V}_1$.

The neglect of magnetism, as well as the shortcomings of the tight-binding approximation, are likely sources for the lack of agreement between the effective pair interactions obtained from electronic structure calculations and those derived from the experimental SRO intensity. Further studies based on spin-polarized and fully self-consistent calculations may be required for a meaningful comparison with the experimental data.

V. CONCLUSION

Diffuse scattering experiments provide a powerful experimental tool to study atomic interactions in alloys and, from them, phase stability as a function of temperature and composition. Furthermore, this type of experimental studies also provide a realistic assessment of the quality and merit of the various theoretical models and numerical calculations that have been implemented over the last few years.

In the present study, the neutron diffuse scattering results for the paramagnetic phase of an Fe-V alloy indicate relatively strong effective pair interactions that extend to at least the fifth neighbor pairs. As a consequence, strong statistical correlations are present even at high temperatures which, for all practical purposes, preclude the analysis of the SRO diffuse intensity by means of the conventional Krivoglaz-Clapp-Moss formula. Higher-order approximations, with the obvious computational penalty, are called for. Here we have used a CRO approximation of the CVM which allows us to extract up to fifth neighbor interactions. We note that the commonly used body-center-cube–octahedron approximation, which does not include fourth neighbor interactions,[33,34] is not adequate for a fully consistent treatment of bcc alloys.

As expected, the analysis of the experimental data in $Fe_{0.804}V_{0.196}$ clearly indicates that near the Curie temperature magnetic effects significantly affect the effective atomic interactions and, thus, chemical short-range order. Thus, a full analysis of the data that explicitly includes magnetic fluctuations would be desirable in order to achieve accurate measurements of chemical and exchange interactions.

Finally, we have compared the effective interactions obtained in this work with the electronic structure calculations of Sluiter and Turchi[20] and found significant disagreement, both in terms of the absolute values and in the general trends. A fluctuation study in k space using a very accurate CVM approximation also shows that these calculated interactions are not in line with our experimental results. It is apparent that, in addition to refinements in the experimental techniques and method of analysis, improvements in the electronic structure calculations beyond the tight-binding approximation will be needed before satisfactory agreement is reached.

ACKNOWLEDGMENTS

J.P. Ambroise is gratefully acknowledged for his help in the Debye-Waller measurements on the 7C2 spectrometer of the Léon Brillouin Laboratory. The work at The University of Texas at Austin was supported by the National Science Foundation under Grant No. DMR-91-14646.

[1] F. Ducastelle and F. Gautier, J. Phys. F **6**, 2039 (1976).
[2] G. Tréglia, F. Ducastelle, and F. Gautier, J. Phys. F **8**, 1437 (1978).
[3] A. Bieber and F. Gautier, Physica B **107**, 71 (1981).
[4] A. Bieber and F. Gautier, J. Magn. Magn. Mater. **99**, 293 (1991).
[5] J.W.D. Connolly and A.R. Williams, Phys. Rev. B **27**, 5169 (1983).
[6] J.M. Sanchez, F. Ducastelle, and D. Gratias, Physica **128A**, 334 (1984).

[7] J.M. Sanchez, Phys. Rev. B **48**, 14013 (1993).
[8] A.A. Mbaye, L.G. Ferreira, and A. Zunger, Phys. Rev. Lett. **58**, 49 (1987).
[9] K. Terakura, T. Oguchi, T. Mohri, and K. Watanabe, Phys. Rev. B **35**, 2169 (1987).
[10] A.E. Carlsson and J.M. Sanchez, Solid State Commun. **65**, 527 (1988).
[11] A. Zunger, S.-H. Wei, A.A. Mbaye, and G.L. Ferreira, Acta Metall. **36**, 2239 (1988).
[12] S. Takizawa, K. Terakura, and T. Mohri, Phys. Rev. B **39**, 5792 (1989).
[13] L.G. Ferreira, S.-H. Wei, and A. Zunger, Phys. Rev. B **40**, 3197 (1989); **41**, 8240 (1990).
[14] J.M. Sanchez, J.P. Stark, and V.L. Moruzzi, Phys. Rev. B **44**, 5411 (1991).
[15] C. Wolverton, G. Ceder, D. de Fontaine, and H. Dreyssé, Phys. Rev. B **48**, 726 (1992).
[16] J.M. Sanchez and J.D. Becker, Prog. Theor. Phys., Suppl. **115**, 131 (1994).
[17] J.M. Sanchez, in *Structural and Phase Stability of Alloys*, edited by F. Mejia-Lira, J.L. Moran-Lopez, and J.M. Sanchez (Plenum, New York, 1992), pp. 151–165.
[18] V. Pierron-Bohnes, M.C. Cadeville, A. Bieber, and F. Gautier, J. Magn. Magn. Mater. **54-57**, 1027 (1986).
[19] M. Hennion, J. Phys. F **13**, 2351 (1983).
[20] M. Sluiter and P.E.A. Turchi, in *High-Temperature Ordered Intermetallic Alloys IV*, edited by L.A. Johnson, D.P. Pope, and J.O. Stiegler, MRS Symposia Proceedings No. 213 (Materials Research Society, Pittsburgh, 1991), p. 37.
[21] P.E.A. Turchi, M. Sluiter, and G.M. Stocks, in *High-Temperature Ordered Intermetallic Alloys IV* (Ref. 20), p. 75.
[22] J.B. Staunton, D.D. Johnson, and F.J. Pinski, Phys. Rev. Lett. **65**, 1259 (1990).
[23] M. Bessière, Y. Calvayrac, S. Lefebvre, D. Gratias, and P. Cénédèse, J. Phys. **47**, 1961 (1986).
[24] B.D. Butler and J.B. Cohen, J. Appl. Phys. **65**, 2214 (1986).
[25] F. Solal, R. Caudron, F. Ducastelle, A. Finel, and A. Loiseau, Phys. Rev. Lett. **58**, 2245 (1987).
[26] F. Solal, R. Caudron, and A. Finel, in *Alloy Phase Stability*, edited by G.M. Stocks and A. Gonis, Vol. 163 of *NATO Advanced Study Institute, Series E: Applied Sciences* (Kluwer Academic, Dordrecht, 1989), p. 107.
[27] B. Schönfeld, L. Reinhardt, and G. Kostorz, Phys. Status Solidi B **147**, 457 (1988).
[28] W. Schweika and H.G. Haubold, Phys. Rev. B **37**, 9240 (1988).
[29] L. Reinhard, B. Schönfeld, G. Kostorz, and W. Bürer, Phys. Rev. B **44**, 1727 (1990).
[30] L. Reinhard, J.L. Robertson, S.C. Moss, G.E. Ice, P. Zschack, and C.J. Sparks, Phys. Rev. B **45**, 2262 (1992).
[31] F. Chassagne, M. Bessière, Y. Calvayrac, P. Cénédèse, and S. Lefebvre, Acta Metall. **14**, 367 (1989).
[32] W. Schweika, *Neutron Scattering for Materials Science*, edited by S.M. Shapiro, S.C. Moss, and J.D. Jorgensen, MRS Symposia Proceedings No. 166 (Materials Research Society, Pittsburgh, 1990), p. 249.
[33] V. Pierron-Bohnes, S. Lefebvre, M. Bessière, and A. Finel, Acta Metall. Mater. **34**, 2701 (1990).
[34] V. Pierron-Bohnes, M.C. Cadeville, A. Finel, and O. Schaerpf, J. Phys. **1**, 1247 (1991).
[35] J.I. Seki, M. Hagiwara, and T. Suzuki, J. Mater. Sci. **14**, 2404 (1979).
[36] I. Mirebeau, M.C. Cadeville, G. Parette, and I.A. Campbell, J. Phys. F **12**, 25 (1982).
[37] S. Lefebvre, F. Bley, and I. Mirebeau (unpublished).
[38] J.W. Cable, H.R. Child, and Y. Nakai, Physica B **156-157**, 50 (1989).
[39] V. Pierron-Bohnes, I. Mirebeau, E. Balanzat, and M.C. Cadeville, J. Phys. F **14**, 197 (1984).
[40] P.J. Brown, H. Capellmann, J. Déportes, D. Givord, and K.R.A. Ziebeck, J. Magn. Magn. Mater. **31-34**, 295 (1983).
[41] V.F. Sears, Neutron News **3**, 26 (1992).
[42] B. Borie and C.J. Sparks, Acta Crystallogr. A **27**, 198 (1971).
[43] J.M. Cowley, J. Appl. Phys. **21**, 24 (1950).
[44] V. Pierron-Bohnes, C. Leroux, J.P. Ambroise, A. Menelle, and P. Bastie, Phys. Status Solidi A **116**, 529 (1989).
[45] D. Gratias and P. Cénédèse, J. Phys. (Paris) Colloq. **46**, C9-149 (1985).
[46] J.M. Sanchez, Physica **111A**, 200 (1982).
[47] M.A. Krivoglaz, *Theory of X-Ray and Thermal Neutron Scattering by Real Crystals* (Plenum, New York, 1969).
[48] P.C. Clapp and S.C. Moss, Phys. Rev. **142**, 418 (1966); **171**, 754 (1968).
[49] S.C. Moss and P.C. Clapp, Phys. Rev. **171**, 764 (1968).